

## DUAL FREQUENCY (25 MHZ, 50 MHZ) SINGLE ELEMENT ANNULAR TRANSDUCER

B. Jadidian, A. A. Winder, and M. Lanagan\*

J&W Medical LLC, 56 Partrick Rd., Westport CT 06880

\*Materials Research Institute, 280 Materials Research Laboratory Building, University Park, PA 16802

### ABSTRACT

A dermatological scanning acoustic microscope (DSAM) is of significant interest for detecting and screening dermatological cancer and environmentally induced diseases. DSAM would also provide a valuable measure of the extent of tissue damage that would impact on surgical planning and the effectiveness of post-surgical therapeutic treatment. A scanning acoustic microscope for *in vivo* imaging and characterization of micro-cellular structures of the skin must utilize a transducer with a beam penetration to at least 1.0 cm and axial/lateral resolutions less than 100  $\mu\text{m}$ . To fulfill these requirements, a comprehensive finite element analysis was performed to design a transducer using piezoelectric *PVDF-TrFe copolymer*, operating at 25 and 50 MHz. The specific resonance frequencies were obtained with appropriate series inductor-tuning. The estimated lateral resolution of the transducer is 40-80  $\mu\text{m}$ . The active element of transducer is composed of 23  $\mu\text{m}$  thick gold-electroded PVDF-TrFe ring that is backed with 4 mm hard epoxy. The insertion loss/bandwidth of the transducer at 25 and 50 MHz were  $-31\text{dB}/99\%$  and  $-26\text{dB}/70\%$ , respectively. The fabrication method and results obtained are presented.

### INTRODUCTION

Skin imaging is an obvious application for acoustic microscopy because the skin is comprised of thin layers of tissue which undergo structural alteration when diseased. High resolution acoustic imaging of skin neoplasms can provide the dermatologist with knowledge unattainable by any other imaging modality. For skin tumors such as basal cell carcinoma, it is essential to know the depth of invasive in order to plan therapy and decrease the rate of local recurrence. Similarly for malignant melanoma, it is important to know the depth of the lesion and its lateral extent in order to create the proper surgical margins.

In the past several years, ultrasound has been used effectively to evaluate subcutaneous tissues, muscles, tendons, peripheral nerves, bursae, and joints. Imaging of the skin has also been performed, but requires very high frequency probes, 20 MHz or greater. With this high frequency ultrasound equipment the epidermis can be distinguished from the dermis, the papillary layer of the dermis can be distinguished from the reticular layer, and blood vessels, tendon sheaths, tendons, ligaments, and adipose tissue can be identified.

In recent years, there have been several notable studies indicating the clinical potential of very high frequency (VHF) acoustic imaging from 20 MHz to 200 MHz. Bamber et al [1] obtained B-scan images at 22 MHz from 16 skin lesions and showed excellent correlation with histology. In particular, acoustic data provided significant information about the internal structure of the tumor, particularly the pattern of collagen structures and keratin. These images were further improved by spatial filtering to reduce speckle content [2]. Foster and his group [3] developed new transducer probes in the range of 40-100 MHz, providing lateral resolution ranging from 20  $\mu\text{m}$  to 75  $\mu\text{m}$ , for clinical applications, including ophthalmic, skin, and intravascular imaging. Lockwood et al [4] developed needle-shaped probes with center frequencies of 45 MHz and 55 MHz, which provided 125  $\mu\text{m}$  lateral, 55  $\mu\text{m}$  axial resolution and 105  $\mu\text{m}$  lateral, 42  $\mu\text{m}$  axial resolution, respectively. The 45 MHz image clearly depicted fibrous plaque in an excised section of human femoral artery and the 55 MHz image of parenchymal tissue in bovine liver depicted vascular structures and the irregular contour of the hepatic vein. Yokosawa et al [5] developed a 120 MHz rod-shaped probe with a lateral resolution of 13  $\mu\text{m}$ . They were able to show the blood vessels and micro-structures that characterize the medulla in a fresh bovine kidney. The same group used the probe to image normal kidney tissue of a living mouse and tumor tissue implanted in another mouse kidney. The ultrasonic images correlated well with the histological sections taken from the imaged organs. Ermert and his group [6] developed a 50-150 MHz ultrasound imaging system for dermatology and ophthalmology. Coded pulse technology was employed to increase the signal-to-noise ratio by 12 dB, at the expense of introducing image artifacts from large temporal sidelobes after compression. Two

commercial broadband transducers, utilizing PZT (90 MHz) and PVDF (50 MHz), were used to cover the one and a half octaves. The images in the 100 MHz range permitted structures, such as sweat glands, hair follicles and skin layers, to be discernible and showed the potential of the VHF range to provide a measure of skin tumor structure.

Most imaging systems operating above 15 MHz utilize a single element transducer made of piezoelectric materials such as lead zirconate titanate (PZT) [7-12], thin film and spin coated PVDF and PVDF-TRFE [13-15], Zinc oxide [5, 16], lead titanate (PT) [17], Lithium niobate ( $\text{LiNbO}_3$ ) [18-20], and piezocomposite [21-26] have already been explored and shown to be appropriate choices for frequency <200 MHz. Due to their excellent piezoelectric properties, lead zirconate titanate (PZT) ceramics have been extensively used in piezoelectric transducers. However because of their high dielectric constant, PZT ceramics must be well matched electrically to the coaxial line and pulser/receiver systems [27]. Therefore, the application of PZT ceramic is limited to frequencies below 100 MHz [3, 28]. Foster et.al. [3] investigated the effect of grain size of PZT ceramics on the material properties and the performance of transducers in the frequency range of 30 to 80 MHz. Using fine and coarse grained PZT ceramics, it was realized that as the thickness of the ceramic resonator approached the PZT grain size, the mechanical losses increased rapidly and thickness coupling coefficient decreased. From this study, one could conclude that fine grained piezoceramics were better choices for the fabrication of transducers resonating >40 MHz. Piezoelectric polymers offer several advantages, including low acoustic impedance and dielectric constant, flexibility, and availability in thin sheets (thickness of 9-110  $\mu\text{m}$ ). However, their high dielectric loss results in low sensitivity.

The specific aim of this study was to fabricate a dual-frequency annular piezoelectric transducer operating in two distinct frequencies, namely 25 and 50 MHz. The following sections represent the organization of this paper. Section II describes the design specifications, material selection, and KLM model. Section III explains the fabrication of annular transducer. Section IV presents the results and discussion. Section V is the conclusions.

## II. DESIGN SPECIFICATIONS, MATERIAL SELECTION, AND KLM MODEL

### A. Design Specifications of Annular Transducer

The annular transducer was configured with only one active annular ring of a piezoelectric material operating at half wavelength mode resonating at 25 and 50 MHz with specific resonances based on separate inductor-tuning. The piezomaterial has an annular ring electrode on its backside and attached to a backing layer while its front face is electroded across its surface. The active piezomaterial is made of P(VDF<sub>0.75</sub>-TrFE<sub>0.25</sub>) copolymer film (23  $\mu\text{m}$  thick, MSI, Wayne, PA) because of its low dielectric loss and high thickness coupling coefficient [29]. The Curie temperature of this commercially available copolymer is approximately 135 °C. Exposing this films to temperatures  $135\text{ }^\circ\text{C} > T > 100\text{ }^\circ\text{C}$  results in a significant loss of their piezoelectric properties. Therefore the maximum temperature use recommended by manufacturer falls in the range of 90 to 100 °C.

To achieve half wavelength mode of operation, the backing layer had to have an acoustic impedance smaller than that of the PVDF-TrFe copolymer ( $Z_{\text{backing layer}} \leq 4.2\text{ MRayls}$ ), sufficient acoustic attenuation to prevent undesired reverberation, and adhere well and directly onto the copolymer film. Using data collected by Wang [30] and measured experimentally in authors laboratory, it was realized that the Epotek 301 was the best candidate as backing layer due to its low acoustic impedance, moderate acoustic attenuation, and good adhesion to the PVDF-TrFe copolymer. In addition Epotek 301 could be easily poured onto the copolymer for direct bonding.

### B. Dynamic Range Considerations

The F-stop number of the acoustic lens, is defined as the ratio of the sphere radius (ROC) to the lens diameter. (In the case of the annular ring, the diameter corresponds to the mean of the inner and outer diameters.). The dimension of the radius was chosen based on dynamic range considerations, which depends on the transducer insertion loss, the absorption losses in tissue and water, and the target strength or reflectivity coefficient at the boundary interfaces. The reflectivity coefficient for water skin

interface is estimated to be about 0.029 (-30.7 dB), skin-fat interface about 0.00608 (-44.4 dB) and fat muscle interface about 0.00761 (-42.4 dB). Assuming a one-way loss of 0.022 dB/mm at 10.0 MHz and a one-way attenuation coefficient of 0.5 dB/cm-MHz<sup>1.3</sup> for skin tissue [31] and a system dynamic range of 95 dB, the estimated absorption losses and potential maximum imaging depth at each frequency would result in the maximum tissue depths.

C. Lateral Resolution and Depth-of-Field

Based on classical diffraction theory, the lateral resolution  $\delta_L$  of the prototype annular transducer can be defined as the -6 dB level of the lateral point response (LPR) of the ultrasound beam, given by  $\delta_L(-6 \text{ dB}) = F \lambda$ , where  $\lambda$  is the wavelength of the longitudinal acoustic wave in water, and the corresponding Depth-of-Field (DOF) in the focal region, expressed as  $\text{DOF} = 7.1 F^2 \lambda$ . This definition of the DOF actually corresponds to the depth over which the 20 dB width of the LPR is maintained within 40-45% of its value in the focal plane. The lateral resolution in the 25-50 MHz range is 40 to 80  $\mu\text{m}$  from a tissue depth of 1 to 10 mm, extending throughout the dermis tissue to the subcutaneous tissue.

D. Design Parameters And KLM Model

The transducer was analyzed using the 1-D KLM model (PiezoCAD; Sonic Concept Inc., Woodinville, WA) using the parameters shown in Table 1. The electrical tuning network is comprised of series inductors with or without a step-down wide-band pulse transformer (2:1 ratio).

Table 1. The design parameters for the modified DSAM transducer array.

<u>Piezoelectric layer</u>	PVDF-TrFe
Thickness ( $\mu\text{m}$ )	22-23
$V_L$ (m/s)	2400
Z (MRayls)	4.5
<u>Electrode layer</u>	Gold
Thickness ( $\mu\text{m}$ )	(front) 88 (back) 150
Annulus Diameters (mm)	4.4 and 8.8
Mean diameter (mm)	6.6
$V_L$ (m/s)	3240
Z (MRayls)	63.8
<u>Backing layer</u>	Epotek-301 epoxy
Thickness (mm)	4.0
$V_L$ (m/s)	2640
Z (MRayls)	3.0
Attenuation (dB/cm-MHz)	3.167
<u>Matching layer</u>	Epotek-301 epoxy
Thickness ( $\mu\text{m}$ )	~18-19
<u>Transducer parameters</u>	
F-Number	1.25
Radius of curvature (mm)	8.25
Center frequency (MHz)	25.3 and 48.7
-6 dB Lateral resolution ( $\mu\text{m}$ )	77.0 @ 25MHz 38.5 @ 50 MHz

In general, the purpose of the matching layer is to protect the front electrode from the environment (e.g., from wear and corrosion). In addition if selected properly, the matching layer can also improve acoustic performance. For best performance, the matching layer should have an acoustic impedance about 2.59 MRayls  $\{(Z_{\text{copolymer}} Z_{\text{water}})^{0.5}$ , where  $Z_{\text{water}} = 1.5 \text{ MRayls}\}$ , have minimum acoustic attenuation for maximum transmission, and adhere well and directly onto the copolymer. Figures 1b and 1c depict the transmission

coefficients of acoustic waves into Epotek 301 through gold layer and into water through the matching layer calculated by [32]:

$$\alpha_{t13} = \frac{4r_{13}}{(r_{13} + 1)^2 \text{Cos}^2 K_2 S + (r_{12} + r_{23})^2 \text{Sin}^2 K_2 S}$$

$$r_{13} = \frac{Z_3}{Z_1}$$

$$r_{12} = \frac{Z_2}{Z_1}$$

$$r_{23} = \frac{Z_3}{Z_2}$$

$$K_2 = \frac{2\Pi}{\lambda_2} = \frac{2\Pi f}{V_2}$$

where  $Z_1, Z_2, Z_3$  are the acoustic impedance of the copolymer, gold or matching layer, and the matching layer or water, respectively. While  $f, V_2,$  and  $S$  are the frequency, longitudinal velocity of the gold or matching layer, and their thickness, respectively.

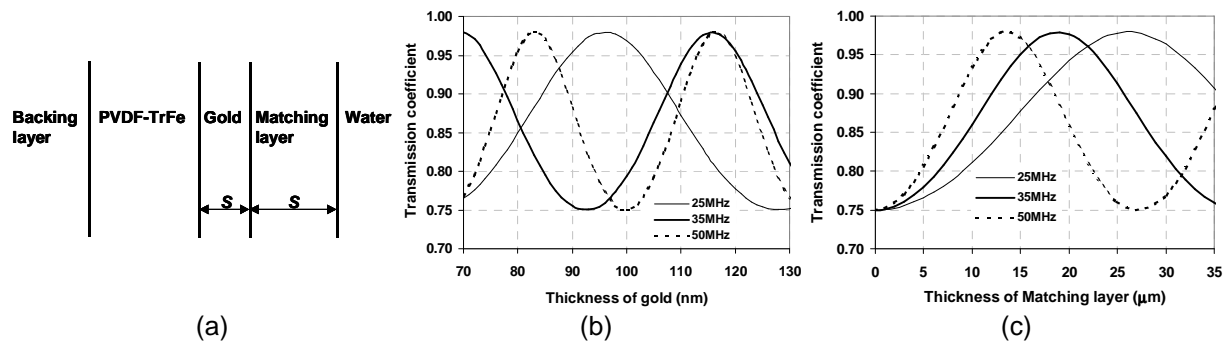


Figure 1. (a) Schematic structure of materials used in the transducer and the transmission coefficient of acoustic waves into (b) matching layer through gold and (c) water through the matching layer.

To achieve maximum transmission at each specific frequency, shown in Figure 1b, the required thickness of gold as front electrode at 25 and 50 MHz are 96µm and 83µm (or 116 µm), respectively. The required thicknesses of matching layer at corresponding frequencies are 13 and 26 µm, respectively. In this study since only one active element is used to generate both desired frequencies, the thickness of the gold front electrode and matching layer have to be optimized for almost equal acoustic transmission at both frequencies. This corresponds to 88 µm or 110 µm thick gold layer and 18-19 µm thick Epotek 301 as matching layer. Notably a gold layer with 88 µm thickness is more preferable for dual frequency mode (25 and 50 MHz) while 110 µm thickness is a better choice for realizing triple frequency mode (25, 35, and 50 MHz).

### III. FABRICATION OF ANNULAR TRANSDUCER

Figure 2 schematically shows the processing steps involved in the fabrication of a 25-50 MHz transducer. The acoustic impedance of gold,  $Z = 63.8$  MRayls [33], is much higher than that of PVDF-TrFe film. Thus to be operated at  $\lambda/2$  resonant-mode, the thickness of the gold layer had to be significantly smaller relative to that of the film [29]. A ~150 nm thin layer of gold was sputtered on the back side of a 8.8 mm in diameter copolymer disc. Then the copolymer was secured onto a Mylar sheet with the gold electrode facing up. A brass ring (13 mm diameter) was placed around the element and Epotek 301 (Billerica, MA) was cast into the gap between the element and the ring. Before casting, the epoxy was partially cured at

room temperature to permit gold electrode to be exposed for wire attachment. After curing, a 120 $\mu$ m thick copper wire was placed onto the epoxy and connected to the gold electrode using silver epoxy (DuPont 4922N, Research Triangle Park, NC) and another wire was soldered to the brass tube. The back side of the element was refilled with Epotek 301 and cured at room temperature. The thickness of the epoxy layer on the back of the polymer film was approximately 4mm and acted as the backing layer. After removing the Mylar sheet, the front face of the sub-transducer was cleaned with alcohol, covered with a 4.4 mm diameter Mylar at its center, and sputtered across with 100 nm thick gold film to form the front electrode. Then it was placed onto a stainless steel ball with a radius of 8.6 mm and pressed while heated at 60 °C to obtain the desired radius of curvature (R-O-C). The inner surface of the brass tube was coated with Epotek-301 to form insulation between the brass housing and the wire attached to the backside of the piezo-copolymer. The front face of the transducer was then immersed in water and its complex impedance, capacitance, and dissipation factor were measured using an impedance analyzer (Agilent 4294A, Santa Clara, CA). An inductor with appropriate value for the desired frequency of 25 MHz was soldered to a wire of a 30 cm long of a three-line cable. Next the copper wire attached to the back electrode was soldered to the inductor and the second wire of the cable. The third wire of the cable was soldered to the wire attached to the brass tube. Then the end of the brass tube was covered and sealed with a 13 mm diameter epoxy disc. The copolymer was repoled for 30 minutes at 75 °C and 120 MV/m electric field applied between the front and back gold electrodes.

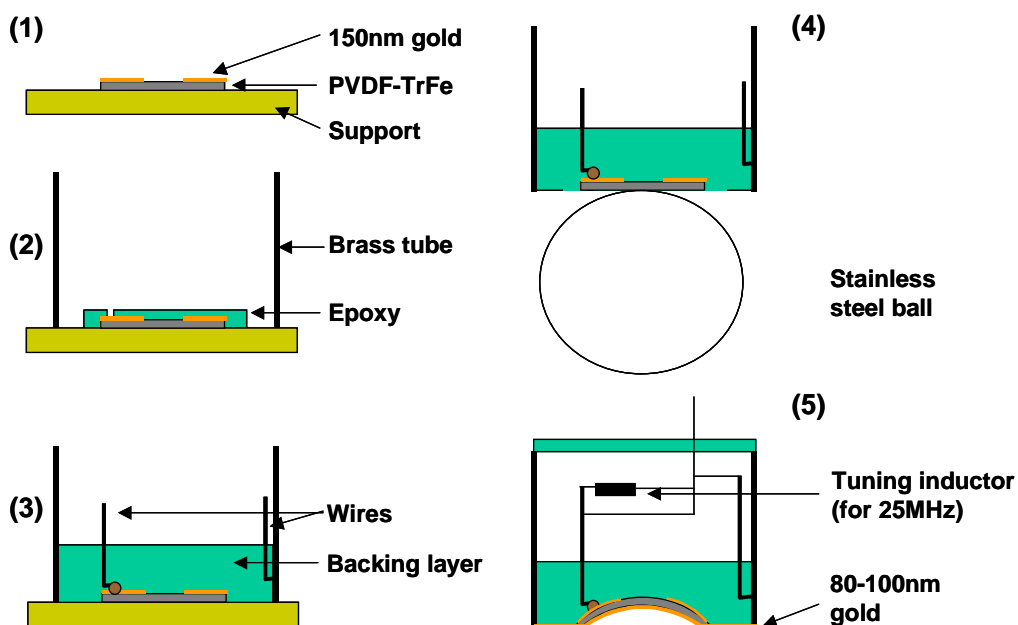


Figure 2. Sub-transducer process steps.

The pulse-echo responses of the transducers were measured using a conventional pulse-echo method in deionized, degassed, and distilled water at room temperature shown in Figure 3a. The transducers were excited at 5 Vp-p by a standard pulser (HP8082A, Hewlett-Packard, Santa Clara, CA). A polished stainless steel plate (10 x 10 x 2.5 cm<sup>3</sup>) was placed at the transducer focal point and the reflected echo waveforms were recorded by a digital oscilloscope (LeCroy 6100, Chestnut Ridge, NY) set at 50- $\Omega$  coupling. Cable lengths between the pulser/transducer and transducer/DSO were 30 cm. The frequency spectrums of the transducer were then obtained by using the Fast Fourier Transform (FFT) function option built-into the oscilloscope. Using the frequency spectrum, the center frequency ( $f_c$ ), maximum frequency ( $f_{max}$ ) and the low as well as the high frequencies ( $f_L$  and  $f_H$ , respectively) at -6dB points were obtained. The Insertion loss was measured using the setup shown in Figure 3b without compensation for losses caused by diffraction and 2-way attenuation in water. In burst mode, the transducer was excited with a 10-cycle sine wave using HP 8116A function generator (Hewlett-Packard, Santa Clara, CA). The reflected waveforms were collected by the Lecroy digital oscilloscope set at 1-M $\Omega$  coupling.

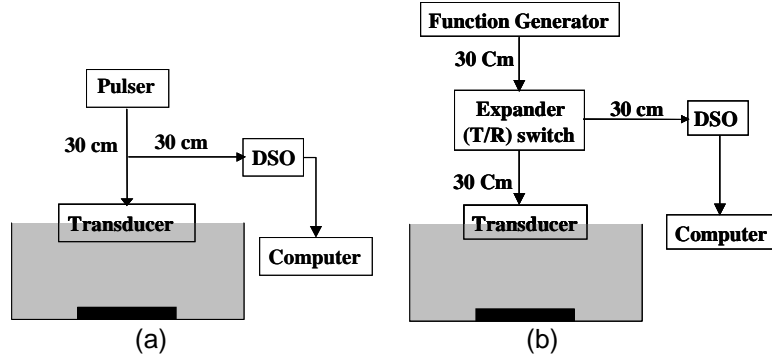


Figure 3. Block diagram for (a) pulsed excitation mode and (b) burst mode.

#### IV. RESULTS AND DISCUSSION

Figure 4 depicts the KLM model of 2-way pulse echo spectral response of the annular transducer based upon a 52 MHz parallel resonance frequency, a 19  $\mu\text{m}$  thick matching layer ( $\lambda/4$  at 35 MHz), tuning inductors producing resonances at 25 and 50 MHz, and a 2:1 pulse transformer. Table 2 compares the bandwidth and insertion loss of the annular transducer, with and without the transformer and matching layer. The addition of matching layer improved pulse echo sensitivity only to about  $\leq 2\text{-dB}$ . This is in good agreement with the predicted improvement (1.7 dB) in acoustic transmission coefficient, shown in Figure 1. Brown [29] reported the addition of a Mylar matching layer onto the front face of 11.8MHz PVDF-TrFEe transducer increased its pulse-echo amplitude (1.2dB) and widened its bandwidth (9%). In this study, similar trend was observed at 50 MHz design frequency. However, for the 25 MHz design, the addition of matching layer gave rise to reducing the bandwidth. The wideband pulse transformer seemed to be primary in optimizing the echo response (insertion loss) at the expense of a significant reduction in bandwidth. As seen, a transducer tuned only with inductors and without matching layer had  $-6\text{dB}$  insertion losses  $< 25\text{ dB}$  and very wide bandwidths at both designed frequencies.

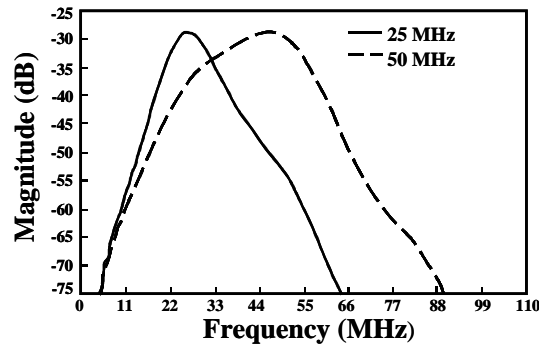


Figure 4. The KLM model of 2-way pulse echo spectral response of the annular transducer resonating at 25 and 50 MHz. The transducer has one matching layer, tuned with inductor and wideband transformer at each frequency.

Table 2. The bandwidth and insertion loss of the annular ring transducer, with and without the pulse transformer and matching layer.

Transformer (2:1) ratio	ML	25 MHz		50 MHz	
		IL (dB)	%BW -6 dB	IL (dB)	%BW -6 dB
√	√	-17.0	46.0	-17.0	59.2
√	×	-19.3	48.5	-18.8	56.6
×	√	-19.9	73.7	-23.2	89.9
×	×	-22.9	93.6	-24.8	77.8

Xfmr: transformer 2:1 ratio, ML: matching layer, IL: insertion loss, BW: bandwidth

Based on the results of KLM analysis, the experimental acoustic characterizations were thus performed on the transducer that did not have matching layer on its front face nor was tuned with a wideband transformer. As described earlier, the transducer was only tuned with one inductor for operation at 25 MHz. Based upon the results shown in Figure 5, the corresponding calculated reactance of the transducer at actual center frequencies of 23.3 and 47.8 MHz were calculated by:

$$X_c = \frac{1}{j\omega C} = \frac{t}{j2\pi f \epsilon_0 \epsilon_r A}$$

where  $f$ ,  $A$ , and  $t$  are the frequency, copolymer active area, and its thickness, respectively. The  $\epsilon_0$  and  $\epsilon_r$  are the permittivity of free space ( $8.85 \times 10^{-12}$  F/m) and relative permittivity, respectively. The transducer reactance values at actual center frequencies of 23.3 and 47.8 MHz were 75 and 51  $\Omega$ , respectively. As described by Sherar and Foster [34], the maximum sensitivity and minimum insertion loss of a transducer is achieved when its reactance is 50  $\Omega$ . Therefore the transducer in this study was only tuned with an inductor for operation at the designed frequency of 25 MHz.

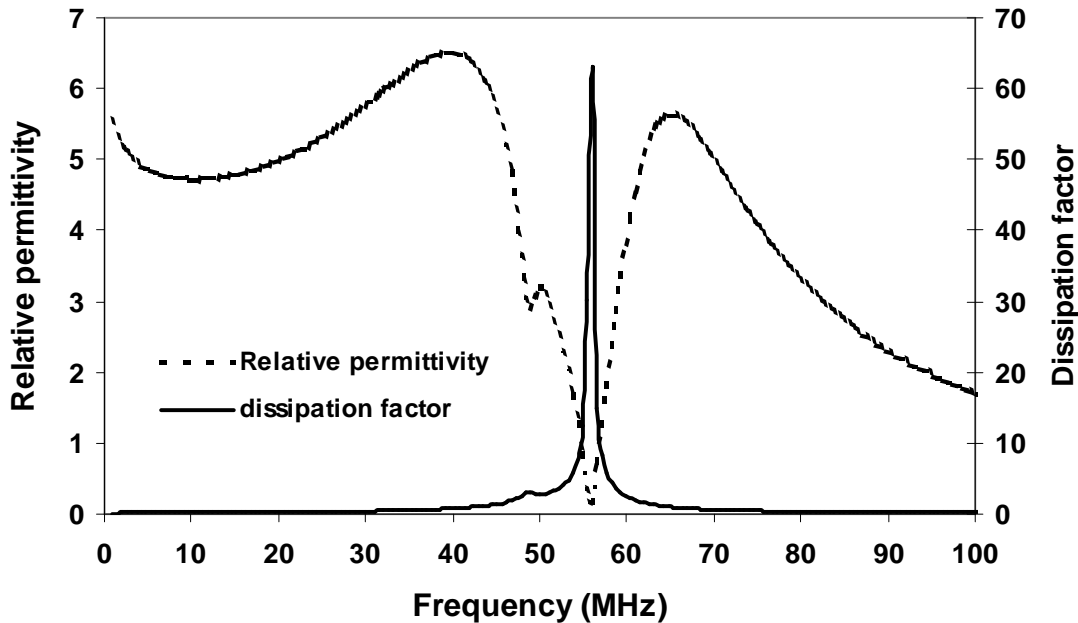
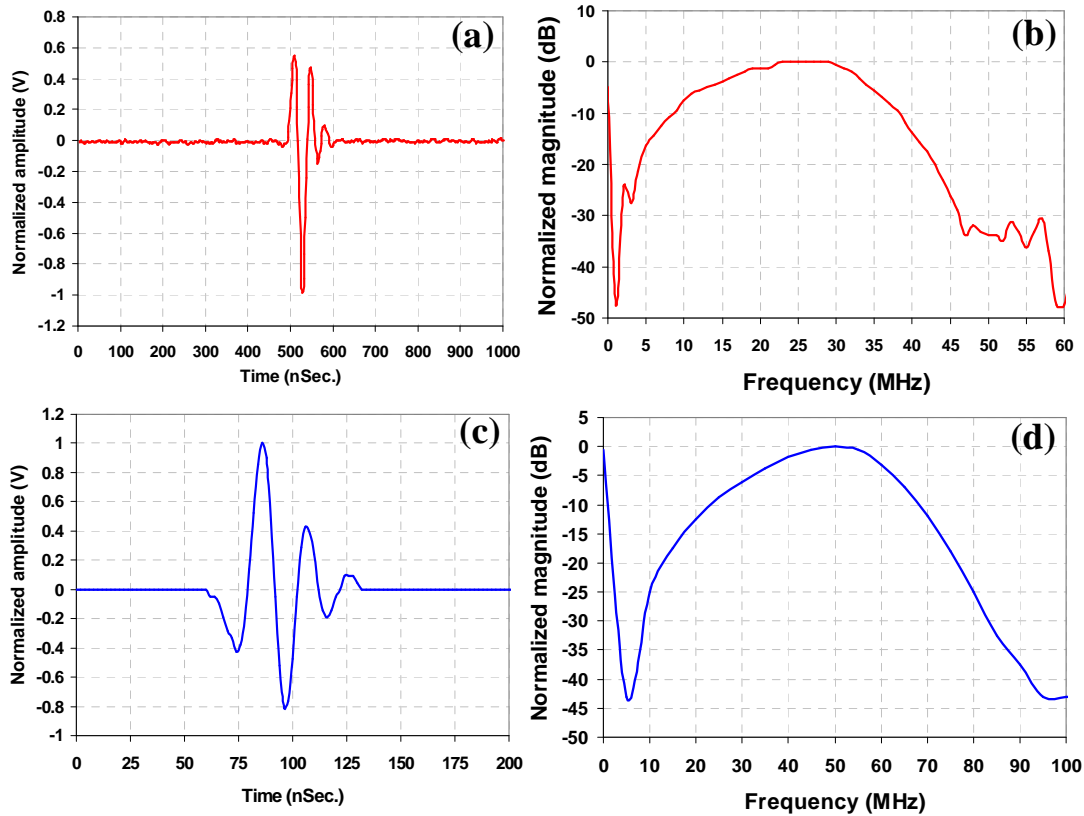


Figure 5. The relative permittivity and dissipation factor of un-tuned transducer immersed in water.

Figures 6(a-b) and 6(c-d) show the measured time domains and normalized frequency spectrums of the annular transducer at 25 MHz and 50 MHz, respectively. Table 3 summarizes the measured parameters. The results obtained at 50MHz are in good agreement with those predicted by the KLM model. Tuned at 25 MHz, the experimental center frequency and peak frequency were 23 MHz and 25 MHz, respectively. The measured and modeled insertion losses were -31 and -23 dB, respectively. Higher insertion loss at this frequency can be attributed to factors. Firstly, the thickness of the gold front electrode might be smaller than 88 nm. Referring to Figure 1b, it is postulated that the gold thickness is about 83 nm giving consequently rise to lower and higher acoustic transmission coefficients at 25 and 50 MHz, respectively.

Secondly, the insertion loss is directly proportional the thickness coupling coefficient of the piezopolymer [35]. The measured  $k_t$  value of the 23  $\mu\text{m}$  thick copolymer is  $\sim 0.31$  around its natural resonance frequency of 47-49 MHz. It is anticipated that higher insertion loss observed during operating at 25 MHz designed frequency is also attributed to the lower thickness coupling coefficient of the copolymer at this frequency. It must be mentioned that there was a good agreement between the KLM modeled and experimental -6dB bandwidths at 25 MHz.



Figures 6. The time domain and normalized frequency spectrums of the annular transducer at designed frequencies of (a-b) 25 MHz and (b-c) 50 MHz.

Table 3. Measured parameters of annular transducer.

Parameter/Frequency	25 MHz		50 MHz	
	Exp.	KLM model	Exp.	KLM model
-6 dB $f_H$ (MHz)	35.0		63.74	
-6 dB $f_L$ (MHz)	11.8		30.58	
-6 dB $f_0$ (MHz)	23.4	25.0	47.16	48.75
-6 dB width (MHz)	23.2		33.16	
-6 dB BW (%)	99.14	93.6	70.29	77.8
Insertion Loss (dB)	-30.99	-22.9	-26.14	-24.8

### V. CONCLUSION

An annular transducer was fabricated to radiate ultrasonic frequencies at 25 MHz and 50 MHz. The active element of the transducer was made of 23  $\mu\text{m}$  thick PVDF-TrFe copolymer in the shape of a ring that was backed with hard epoxy. The KLM model was performed to determine the performance of the transducer. The parameters analyzed were the active area of the copolymer, thickness of the front and back electrodes, thickness of the backing and matching layer, and the transducer F-number. It was realized that the bandwidths and insertion losses of the transducer at the designed frequencies were about 78-95% and <-24dB. Very good agreements were observed between the experimental measurements and those predicted by the KLM model. The active area of the copolymer was chosen such that the transducer only needed to be tuned with an inductor for 25 MHz frequency. The insertion loss/-6dB bandwidth at 25 MHz and 50 MHz were -23dB/99% and -26dB/70%, respectively.

## References

1. J. C. Bamber, Harland, B.A. Gusterson, P.S. Mortimer, "Correlation between histology and high resolution echographic images of small skin tumors", *Acoustic Imaging*, 19, pp. 369-374, 1992,.
2. J. C. Bamber, D.C. Crawford, D.A. Bell, C.C. Harland, B.A. Gusterson, P.S. Mortimer, *Acoustic Imaging*, Volume 19, Edited by H.Ermert and H.P. Harjes, Plenum Press, New York 1992, 447-452.
3. F. S. Foster, L. K. Ryan, and D. H. Turnbull, "Characterization of lead zirconate titanate ceramics for use in miniature high frequency (20-80 MHz) transducers," *IEEE Trans. Ultrason., Ferroelectric., Freq. Contr.*, vol. 38, no. 5, pp. 446-453, 1991.
4. G. R. Lockwood, L. K. Ryan, and F. S. Foster, "A 45 to 55 MHz needle-based ultrasound system for invasive imaging", *Ultrasonic Imaging*, 15, pp. 1-13 (1993).
5. K. Yokosawa, R. Shinomura, S. Sano, Y. Ito, S. Ishikawa, and Y. Sato, "A 120 MHz probe for tissue imaging," *Ultrasonic Imaging*, 18, pp. 231-239, 1996.
6. M. Vogt, K. Kaspar, P. Altmeyer et al, "High frequency ultrasound for high resolution skin imaging", *Frequenz*, 54, pp. 12, 2000.
7. M. Lukacs, M. Sayer, and F. S. Foster, "Single element high frequency (<50 MHz) PZT sol gel composite ultrasound transducers," *IEEE Trans. Ultrason., Ferroelectric., Freq. Contr.*, vol. 47, no. 1, pp. 148-159, 2000.
8. M. I. Zipparo, K. K. Shung, and T. R. Shrout, "Piezoceramics for high frequency (20-100 MHz) single element imaging transducers," *IEEE Trans. Ultrason., Ferroelectric., Freq. Contr.*, vol. 44, no. 5, pp. 1038-1048, 1997.
9. G. R. Lockwood, D. H. Turnbull, F. S. Foster, "Fabrication of high frequency spherically shaped ceramic transducers," *IEEE Trans. Ultrason., Ferroelectric., Freq. Contr.*, vol. 41, no. 2, pp. 231-235 1994.
10. Q. Zhou, J. M. Cannata, R. J. Meyer, Jr., D. J. Van Tol, S. Tadigadapa, W. J. Hughes, K. K. Shung, and S. Troler-McKinstry, "Fabrication and characterization of micromachined high-frequency tonpizl transducers derived by PZT thick films," *IEEE Trans. Ultrason., Ferroelectric., Freq. Contr.*, vol. 52, no. 3, pp. 350-357, 2005.
11. Q. Q. Zhang, F. T. Djuth, Q. F. Zhou, C. H. Hu, J. H. Cha, K. K. Shung, "High frequency broadband PZT thick film ultrasonic transducers for medical imaging applications," *Ultrasonics*, 44, pp. e711-e715, 2006.
12. T. W. Button, S. Cochran, K. J. Kirk, D. MacLennan, A. MacNeil, K. McDonald, C. Meggs, D. Rodriguez-Sanmartin, R. Webster, and D. Zhang, "Net-shape ceramic manufacturing as an aid to realize ultrasonic transducers for high-resolution medical imaging," *The Proc. IEEE Int. Symp. UFFC*, pp. 1625-1628, 2005.
13. L.F. Brown, RL. Carlson and J.M. Sempsrott, "Spin-cast P(VDF-TrFE) films for high performance medical ultrasound transducers," *The Proc. IEEE Int. Symp. UFFC*, pp. 1725-1727, 1997.
14. J. A. Ketterling, O. Aristizabal, D. H. Turnbull, and F. L. Lizzi, "Design and fabrication of a 40-MHz annular array transducer," *IEEE Trans. Ultrason., Ferroelectric., Freq. Contr.*, vol. 52, no. 4, pp. 672-681, 2005.
15. W. Zou, S. Holland, K. Y. Kim, W. Sachse, "Wideband high frequency line-focus PVDF transducer for materials characterization," *Ultrasonics*, 41, pp. 157-161, 2003.
16. Y. Ito, K. Kushida, H. Kanda, H. Takeuchi, K. Sugawara, and H. Onozato, "Thin-film ZnO ultrasonic transducer arrays for operation at 100 MHz," *Ferroelectrics*, 134, pp. 325-330, 1992.
17. R. Meyer, R. Newnham S. Alkoy, T Ritter, and J. Cochran Jr., "Pre-focused lead titanate >25 MHz single-element transducers from hollow spheres," *IEEE Trans. Ultrason., Ferroelectric., Freq. Contr.*, vol. 48, no. 2, pp. 488-493, 2001.
18. D.A. Knapik, B. Starkoski, C.J. Pavlin, and F.S. Foster, "A realtime 200 MHz ultrasound B-scan imager," *The Proc. IEEE Int. Symp. UFFC*, pp. 1457-1460, 1997.
19. D. A. Kapik, B. Starkoski, C. J. Pavlin, F. S. Foster, "A 100-200 MHz ultrasound biomicroscope," *IEEE Trans. Ultrason., Ferroelectric., Freq. Contr.*, vol. 47, no. 6, pp. 1540-1549, 2000.
20. J. Cannata, A. Ritter, Wo-Hesing Chen, R. H. Silverman, and K. K. Shung, "Design of efficient, broadband single-element (20-80 MHz) ultrasonic transducers for medical imaging," *IEEE Trans. Ultrason., Ferroelectric., Freq. Contr.*, vol. 50, no. 11, pp. 1548-1557, 2003.
21. R. Liu, K. A. Harasiewicz, and F. S. Foster, "Interdigital pair bonding for high frequency (20-50 MHz) ultrasonic composite transducers," *IEEE Trans. Ultrason., Ferroelectric., Freq. Contr.*, vol. 48, no. 1, pp. 299-306, 2001.

22. T. A. Ritter, K. K. Shung, R. T. Tutwiler, and T. R. Shrout, "Medical imaging arrays for frequencies above 25 MHz," *The Proc. IEEE Int. Symp. UFFC*, pp. 1203-1207, 1999.
23. R. Meyer Jr., S. Alkoy, and R. Newnham, "Development of materials and composites for >25 MHz single element transducers," *The Proc. IEEE Int. Symp. UFFC*, pp. 1299-1302, 1999.
24. A. Nguyen-Dinh, L. Ratsimandresy, P. Mauchamp, R. Dufait, A. Flesch, M. Lethiecq, "High frequency piezo-composite transducer array designed for ultrasound scanning applications," *The Proceedings of IEEE symposium*, p. 943-947, 1996.
25. J.-Z. Zhao, C. H. F. Alves, K. A. Snook, J. M. Cannata, W.-H. Chen, R. J. Meyer Jr., S. Ayyappan, T. A. Ritter, K. K. Shung, "Performance of 50 MHz transducers incorporating fiber composite, PVDF,  $\text{PbTiO}_3$  and  $\text{LiNbO}_3$ ," *The Proc. IEEE Int. Symp. UFFC*, vol. 2, pp 1185-1190, 1999.
26. K. Li, H. L. W. Chan, and C. L. Choy, "Samarium and manganese-doped lead titanate ceramic fiber/epoxy 1-3 composite for high-frequency transducer application," *IEEE Trans. Ultrason., Ferroelectric., Freq. Contr.*, vol. 50, no. 10, pp. 1371-1376, 2003.
27. M. Lethiecq, G. Feuillard, L. Ratsimandresy A. Nguyen-Dinh, L. Pardo, J. Ricote, B. Andersen, C. Millar, "Miniature high frequency array transducers based on new fine grain ceramics," *The Proceedings of IEEE Symposium*, pp.1009-1013, 1994.
28. F. S. Foster, C. J. Pavlin, G. R. Lockwood, L. K. Ryan, K. A. Harasiewicz, L. R. Berube, and A. M. Rauth, "Principles and applications of ultrasound backscatter microscopy," *IEEE Trans. Ultrason., Ferroelectric., Freq. Contr.*, vol. 40, no. 5, pp. 608-617, 1993.
29. Lewis F. Brown, "Design considerations for piezoelectric polymer ultrasound transducers," *IEEE Trans. Ultrason., Ferroelectric., Freq. Contr.*, vol. 47, no. 6, pp. 1377-1396, 2000.
30. H. Wang, T. Ritter, W. Cao, K. K. Shung, "High frequency properties of passive materials for ultrasonic transducers," *IEEE Trans. Ultrason., Ferroelectric., Freq. Contr.*, vol. 48, no. 1, pp. 78-84, 2001.
31. C.M.W. Daft, G.A.D. Briggs, and W.D. O'Brien, Jr., "Frequency dependent of tissue attenuation measured by acoustic microscopy", *J. Acoust. Soc. Am.*, 85 (5), pp. 2194-2201, 1989.
32. A. A. Winder, Internal technical memorandum
33. A. R. Selfridge, "Approximate material properties in isotropic materials," *IEEE Trans. On Sonics and Ultrasonics*, vol. 32, no. 3, pp. 381-394, 1985.
34. M. D. Sherar and F. S. Foster, "The design and fabrication of high frequency poly(vinylidene fluoride) transducers", *Ultrasonic Imaging*, 11, pp. 75-94, 1989.
35. K. A. Snook, Jian-Zhong Zhao, C. H. F. Alves, J. M. Cannata, Wo-Hsing Chen, R. J. Meyer Jr., T. A. Ritter, and K. K. Shung, "Design, Fabrication, and evaluation of high frequency, single-element transducers incorporating different materials," *IEEE Trans. Ultrason., Ferroelectric., Freq. Contr.*, vol. 49, no. 2, pp. 169-175, 2002.